THE ARCHIVES OF TRANSPORT

VOL. XXII NO 1 2010

Vibrations of Railroad Due to The Passage of The Underground Train

Robert Konowrocki*
Czesław Bajer**

Received November 2009

Abstract

In the paper we present results of vibration measurements in the train and on the base of the railroad in tunnels of Warsaw Underground. Measurements were performed at straight and curved sections of the track. The paper is focused on the influence of the lateral slip in rail/wheel contact zone on the generation of vibrations and a noise. Vibrations were analyzed in terms of accelerations, velocities or displacements as a function of time and frequency. Results ware compared with the experiment of rolling of the wheel with lateral sleep. In both cases we observed double periodic oscillations.

Keywords: dynamic train-track interaction, ground borne vibrations, curved and straight track, rolling

1. Introduction

One of the most important aspects of underground transportations are judged by the protection of the nearby environment. An increasing interest in the scientific world in the issue of ground borne vibrations from railway tracks is observed. The important question is how they can be controlled through the vehicle/track structure [1]. A wide range of different track and train structures is available, giving different levels of the performance. The underground train creates vibrations which are transmitted thought the track to the ground, and results in reflections and re-radiation of noise to nearby buildings (Fig. 1). The amplitude of vibrations depends on various factors: the wheel and rail roughness, the dynamic properties of the

* Institute of Fundamental Technological Research (IPPT PAN), Warsaw, Poland
** Institute of Fundamental Technological Research (IPPT PAN), Warsaw, Poland

train, train-track wave coupling, properties of the railway track, the vehicle speed, damping properties of soil and propagation of waves thought it [2÷10]. Especially, the rigidity of the underground track base is higher than the classical train track. The speed of the train is relatively lower underground.

We can assume that the railway is an environment friendly mean of transport. In spite of this fact the damaging factors that are mostly the noise and vibration nuisance have to be decreased.

The paper is focused on the influence of the lateral slip in rail/wheel contact zone on the generation of vibrations and a noise. Experimental and theoretical analysis of dynamic phenomena of the wheel or the wheelset rolling over the rail or the track, with slip effects prove double periodicity of lateral motion of the wheel [12]. The kind of lateral motion of the wheel can increase amplitudes of vibration, generated by passage of the train in the underground tunnel. Moreover, two frequencies which differs slightly each other, are highly burdensome, much more than a single frequency of the appropriately higher energy. That is why we will concentrate our investigation on this type of vibrations.

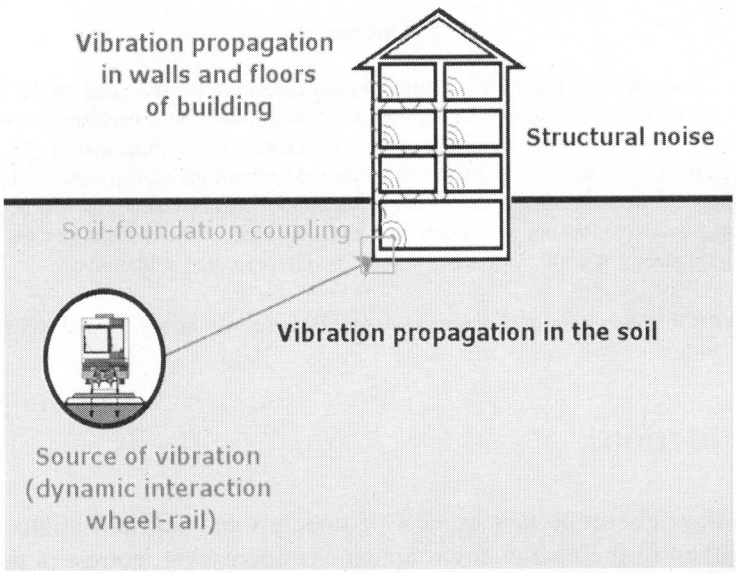

Fig. 1. Ground borne noise generation mechanism

2. Measurements of vibrations

We started from measurements of vibrations in a real train track. The measurement system used in experimental investigations can be divided into three subsystems. The first one allowed us to measure vibrations on the railway track. The

second one can measure vibrations in the nearby building and the third one allows us to register vibrations on the floor inside the train car-body.

The first system included: the temperature sensor, two-axis vibration transducer, GSM receiver, the analog-digital converter 10bit/10kHz, and the computer for data acquisition (Fig. 2). The second system included: two-axis vibration transducer, GSM transmitter, geophone, infrared gate system, analog-digital converter 10bit/10kHz, and the data acquisition computer. The third system was composed of two one-axis transducers and the mobile A/D converter of 12bit/20kHz. The converter contained own data acquisition system. The transducers were fixed to a steel bar for better transmission of vibrations. The bar was localized on the floor of the car-body above a bogie of the car.

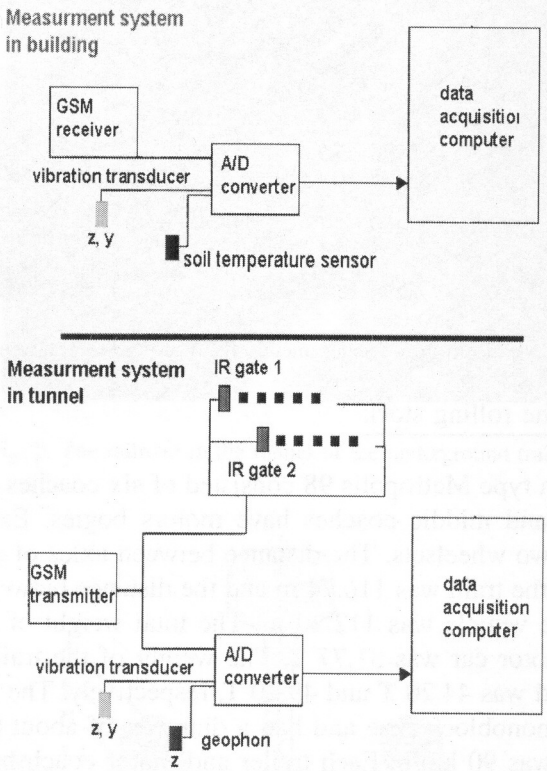

Fig. 2. Scheme of the measurement systems in the tunnel and in the building

How does the measuring system work? The two-axial accelerometer (Fig. 3) mounted on the base of the railroad was connected with the data acquisition computer through the A/D converter. The measurement was initialized and stopped when the infrared gate system gave a starting impulse to the converter. The first infrared gate switched on the converter when the train arrived the measuring area while the

second gate stopped measurements when the train was leaving it. In the same time a GSM transmitter gave an impulse to the GSM receiver located in the building and the second measurement system started recording data on the basement in the building.

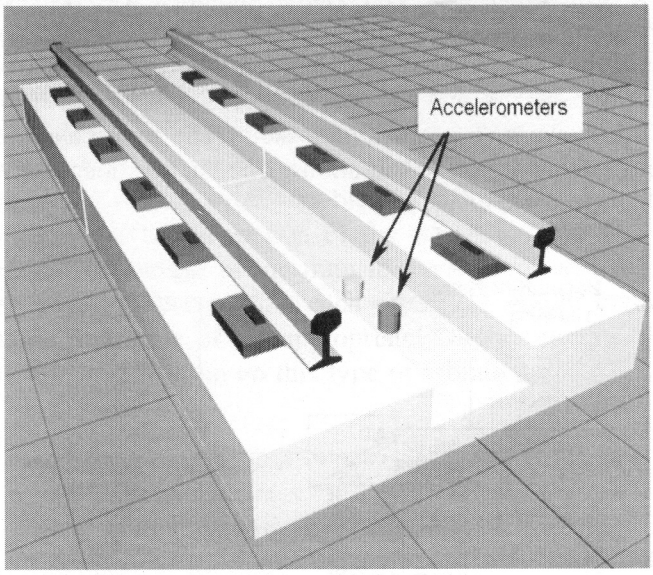

Fig. 3. Localization of accelerometers fixed to the base between rails

Characteristics of the rolling stock

The metro train type Metropolis 98 consisted of six coaches. Two final coaches had trailer bogies and middle coaches have motors bogies. Each coach had two bogies, each with two wheelsets. The distance between axles of a bogie was 2.0 m. The total length of the train was 116.74 m and the distance between the first and the last wheelset of the vehicle was 112.20 m. The total weight of the trailer car was 28.17 T and the motor car was 31.77 T. The weight of the trailer and motor cars with maximum load was 44.20 T and 49.20 T, respectively. The traction and trailer wheels were of a monoblock type and had a diameter of about 0.86 m. Maximum speed of the train was 90 km/h. Each trailer and motor coach had a space for 249 and 229 passengers, respectively. The Fig. 4 shows the train of Metropolis 98 type manufactured by Alstom.

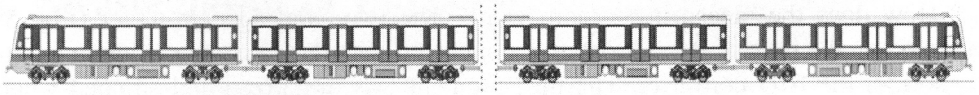

Fig. 4. The train Metropolis 98

Characteristic of a tunnel and a railroad of the underground train

Measurements were performed in a tunnel with a cast iron lining at a depth of about 4-6 m below the ground surface. The tunnel had external radius of 2.6 m. The railroad of underground in the tunnel was a single track type. The track was a non-ballasted concrete slab type (Fig. 5). The UIC60 rails were supported by 5 mm thick rail pads and were fixed by a fastening system Skl 12 (Fig. 6) to non-ballasted concrete slab of about 3 m length. The radius of the curvature of the tested track segment was 1800 m.

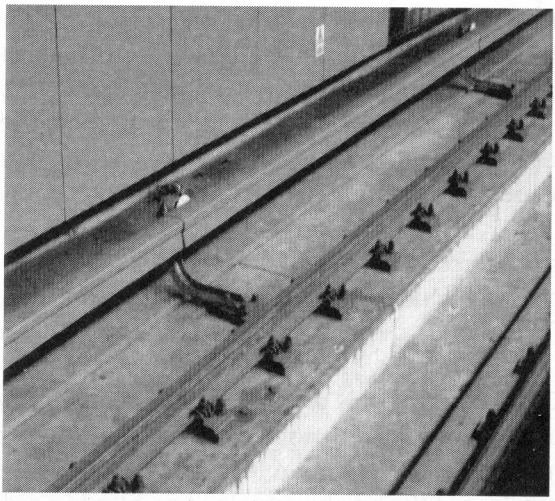

Fig. 5. The railroad in the tunnel of the underground train

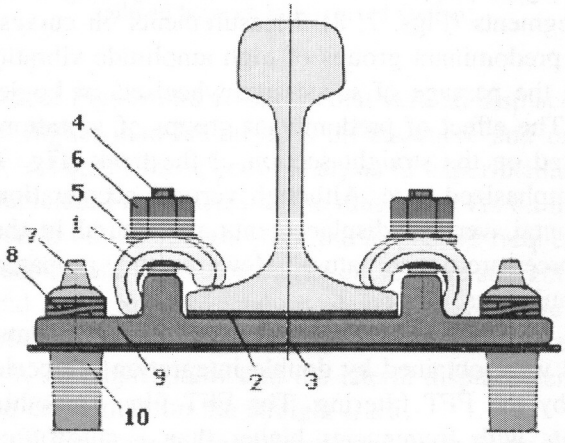

Fig. 6. The fastening system used in the railroad in underground

The fastening system used in the railroad includes: spring clamps (1), rail pad (2), baseplate pad (3), bolt (4), washer (5), nut (6), screw 42 R (7), spring ring Pds 25a (8), baseplate (9), and dowel (10).

Experimental measurements in a tunnel of underground

The vibration measurements were performed for passages of metro train through measurements points. Vibrations were measured within twenty four hours. First measurement points were location on the base of railroad (Fig. 3) on straight and curved test segments of a track in the tunnel. The second one was placed on the floor of the train and measured vibration during the passage by the first measurement points. The third one was located in the building at a distant of about 10 m from the axis of the underground tunnel. The ranges of a speed of the railway vehicle on the curved and straight segments of the track were equal to 48÷58 km/h and 53÷62 km/h, respectively. The vertical and horizontal accelerations and vertical velocity were measured in the tunnel by two-axial accelerometer and one-axial geophone.

Vibrations were analyzed in terms of accelerations, velocities or displacements as a function of time and frequency. The displacements were obtained by integration of accelerations. Then they were verified by integrated velocities obtained by the geophone.

The Savitzky-Golay filtering was used to smooth experimental results. The main idea of the filter was to fit various polynomials to the data surrounding each selected data point. The smoothed curve is determined by replacing each initial data point with the values taken from fitting polynomials. The filtering reduced the distortion of essential features of the data, like peak heights and a noise level of the equipment.

Figures below show vibrations measured in a tunnel. Comparison of experimental results exhibits higher amplitudes of accelerations generated on curves of a track than on straight segments (Figs. 7, 8). Measurements on curves exhibited twenty four characteristic predominant groups of high amplitude vibrations. These groups corresponded with the passage of successive wheelsets of bogies by the point of the measurement. The effect of predominant groups of vibrations do not occur in the results registered on the straight section of the track (Fig. 9). This important feature must be emphasized here. Although vertical accelerations are three times higher than horizontal, vertical displacements are natural in the case of vertical load, Horizontal forces are not so natural. However, they propagate with significant intensity towards buildings.

In Figs. 9 and 10 we show vertical and lateral displacements of the basement. The displacements were obtained by double integration of accelerations and additional smoothing by the FFT filtering. The FFT filter smoothing stage removed Fourier components with frequencies higher than a cutoff frequency. We used $f_{cutoff} = 1/n\Delta t$, where n is the number of data points specified by the user (in our case n=19), and Δt is the time spacing between two adjacent data points.

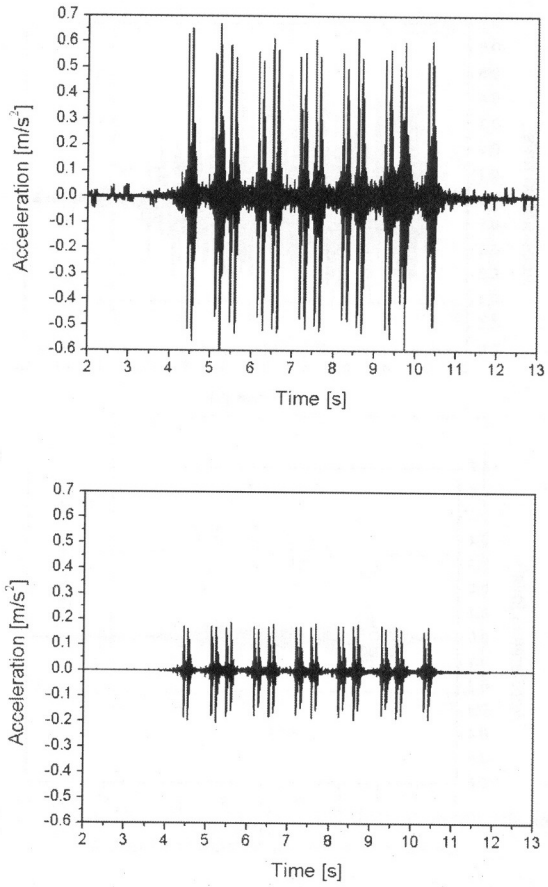

Fig. 7. Time history of vertical (top) and lateral (bottom) accelerations measured on the base of railroad between rails (curved section)

The comparison of Figs. 9 and 10 shows that vertical displacements were about two and five times higher than lateral ones on the curve and on the straight sections, respectively. In Fig. 11 the spectral analysis of experimental results of lateral displacements is depicted. Frequencies of the range 1÷3 Hz on the curved segment can be noticed whereas on the straight track the respective frequency range is equal to 1÷2 Hz. The predominant frequency on the curved and straight segments of track is equal to 1 Hz and 2 Hz. Spectral analysis showed us a double periodicity of the base motion in both cases with low contribution of the third frequency (Fig. 11). Diagrams in Figs. 9, 10 (right) show that the lateral displacements were about 3.5 times higher on the curve than on the straight track.

Although the rolling contact was investigated intensively during last decade, experimental investigations of the problem of skew rolling were rarely performed. Tests on a stand allowed us to prove double periodicity of the lateral motion of the

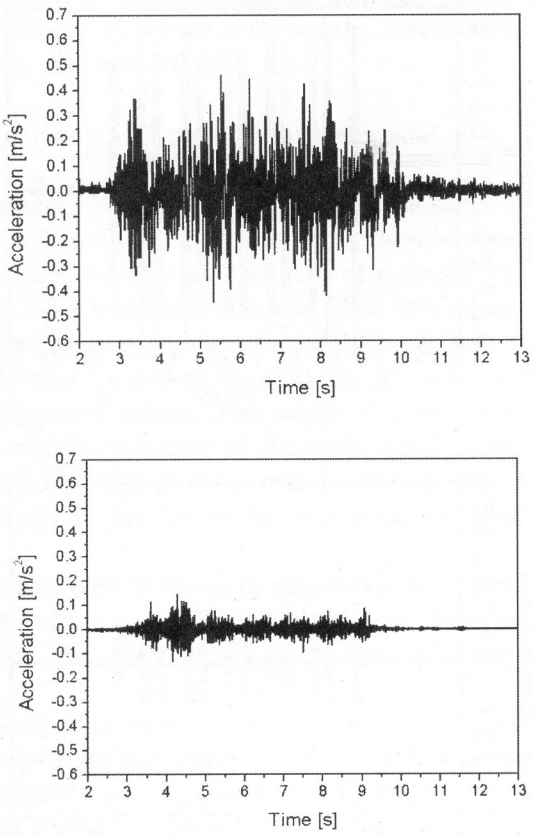

Fig. 8. Time history of vertical (top) and lateral (bottom) accelerations measured on the base of a railroad, in a point between rails (straight section)

wheel at the laboratory level (Fig. 12) [12, 13]. In certain cases a contribution of the third frequency of lower amplitude could be observed. It appeared in he case of a steel instead of polyamide or aluminium in a friction pair. Several factors influenced the lateral motion of the wheel in time. The most contributing factor was the angle between the wheel plane and the track axis (Fig. 13), the rolling speed and the contact pressure (Fig. 14). Unexpectedly the friction pair and the friction law had marginal influence. The theoretical analysis of a phenomenon and the theoretical model elaborated to simulate time characteristics and phase diagrams allowed us to say that two-degree-of freedom system is a sufficient model of a wheel rolling over the rail (track). In each case the double periodicity of lateral motion of the wheel was a characteristic feature. They occur in rolling of the wheel both on the straight rail and on curved sections of the track. We notice identity of vibrations in the laboratory scale (Fig. 12) and on the real track (Fig. 15). Oscillations on curved rails are similar to the shimmy phenomenon. The nature of oscillations in

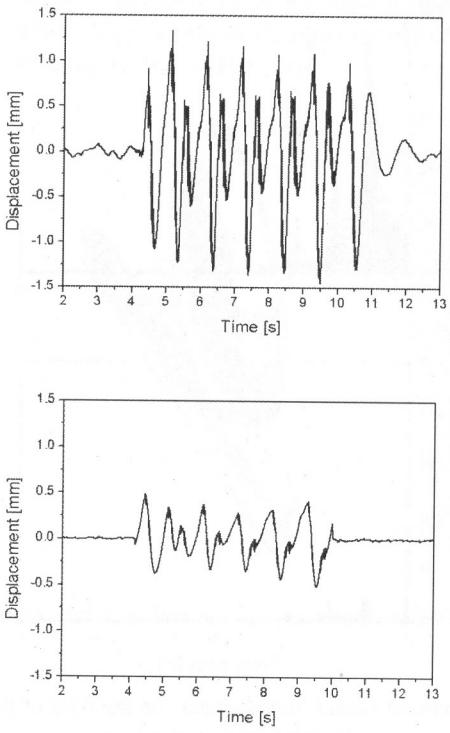

Fig. 9. Time history of vertical (top) and lateral (bottom) displacements on the base of a railroad, in a point between rails (curved section)

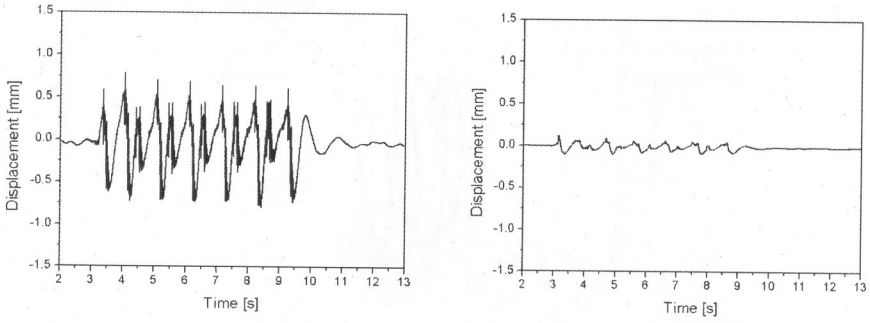

Fig. 10. Time history of vertical (left) and lateral (right) displacements on the base of a railroad, in a point between rails (straight section)

both cases is, however, different. The difference of curvature radiuses of both rails and rotatory oscillations of the wheelset result in a lateral slip. Slope wheel plane

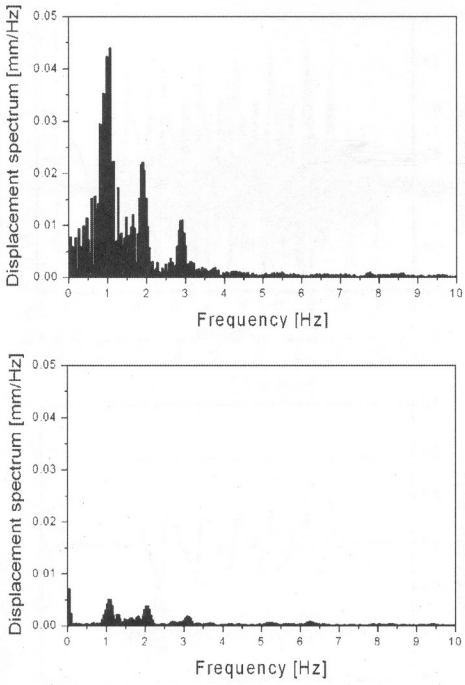

Fig. 11. Comparison of spectra of lateral displacements on the base of the curved (top) and straight (bottom) section of a track

related to temporal rolling direction results in slip oscillation in the contact between wheel and rail. They influence the wear and increase a noise emission.

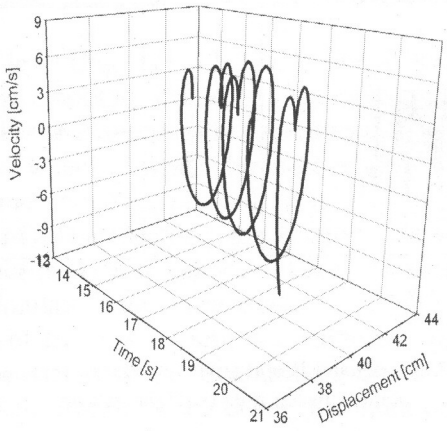

Fig. 12. Phase trajectory for lateral motion of skew rolling steel wheel taken from the experimental stand [13]

In the real track the double periodicity of the lateral motion is noticed in Fig. 9. Both vertical and horizontal components of displacements exhibit higher amplitudes of displacements than on straight lines (Fig. 10).

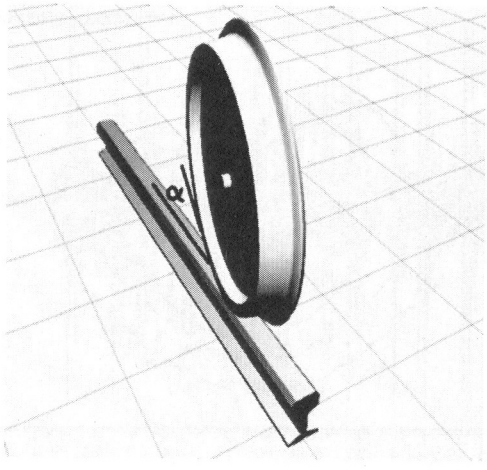

Fig. 13. Skew wheel rolling, resulting in two-periodic vibrations

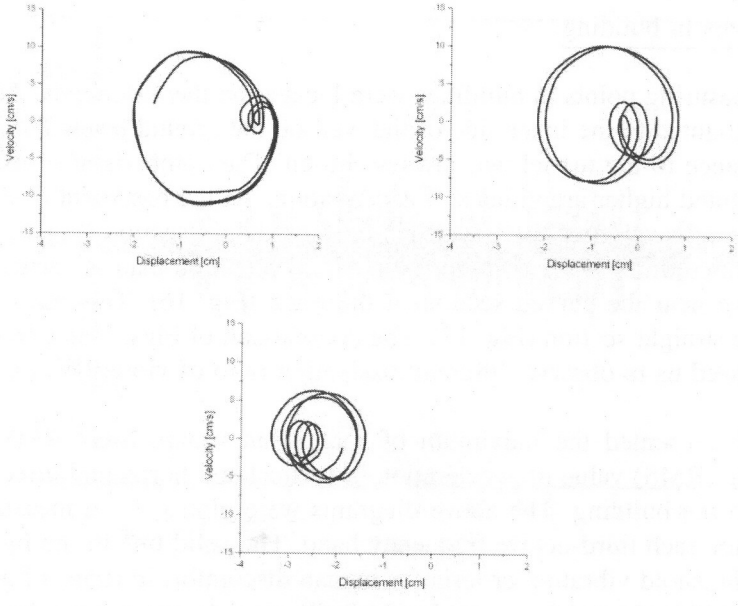

Fig. 14. Phase trajectory for lateral motion taken from the experiment for low, moderate and high vertical contact force [13]

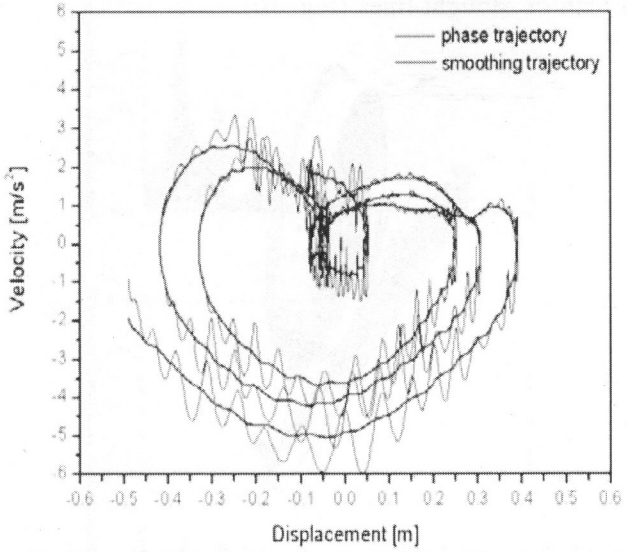

Fig. 15. Phase diagram for lateral motion of base of railroad on the curved section of the track

Measurements in building

The measuring points in buildings were located on the basements. Accelerometers were mounted to the inner side of the wall on the ground level. The wall in the nearest distance to the tunnel was always chosen. The comparison of experimental results exhibited higher amplitudes of accelerations on the basement of the building near the curved section of the track than on the straight section (Figs. 16, 17). We can notice three times lower amplitudes in lateral direction than in vertical direction in a building near the curved section of the track (Fig. 16). This ratio is equal to 1.5 near the straight section (Fig. 17). The comparison of Figs. 7 and 16 or Figs. 11 and 18 allowed us to observe different dissipation ratio of vibration in a soil (about 60 times).

Fig. 20 presented the maximum of root mean square (max RMS) and root mean square (RMS) value of acceleration in vertical and horizontal direction on the basement in the building. The above diagrams were plotted from measurements in a building for each third-octave frequency band. The solid line in the figures corresponds to threshold vibration criteria for human discomfort in terms of acceleration (PN-88/B-02171). In the figure the level of vibration do not exceed the criteria for human discomfort in vertical and horizontal direction.

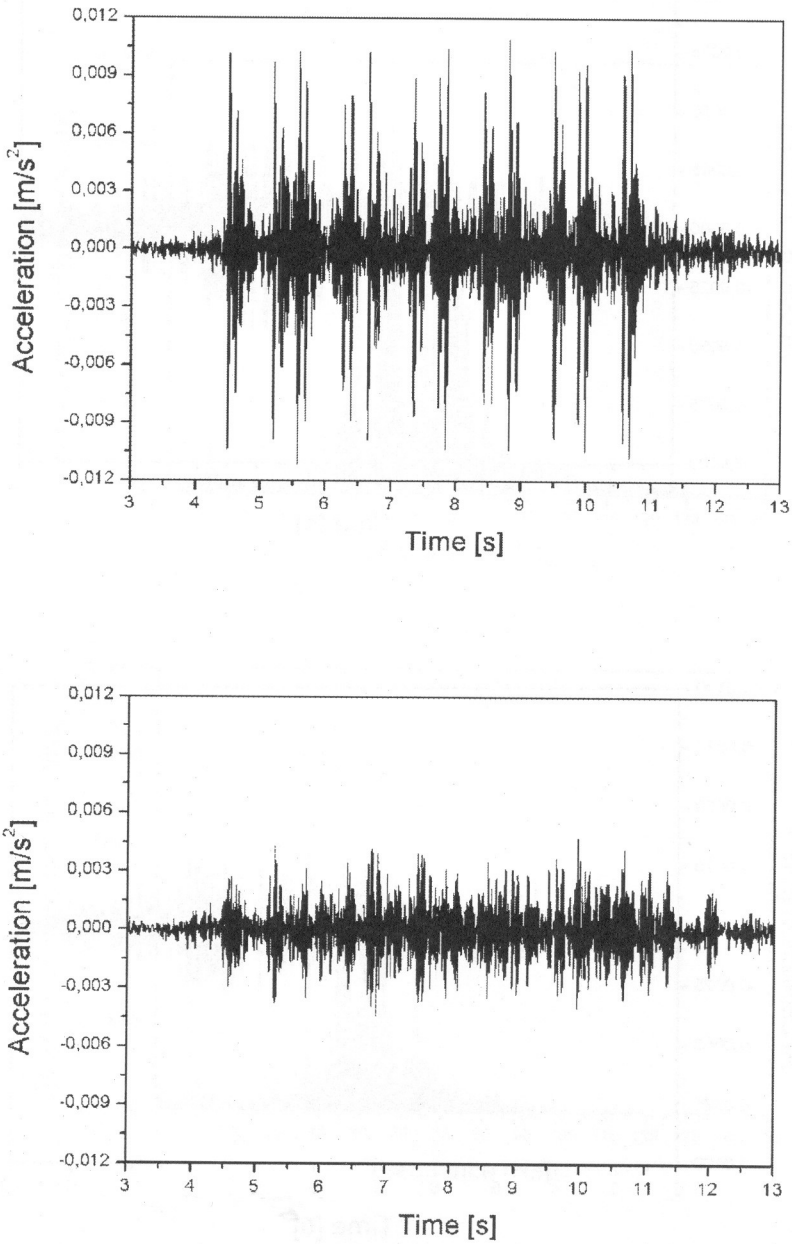

Fig. 16. Time history of vertical (top) and lateral (bottom) accelerations measured on the basement in the building near the curved section of the track

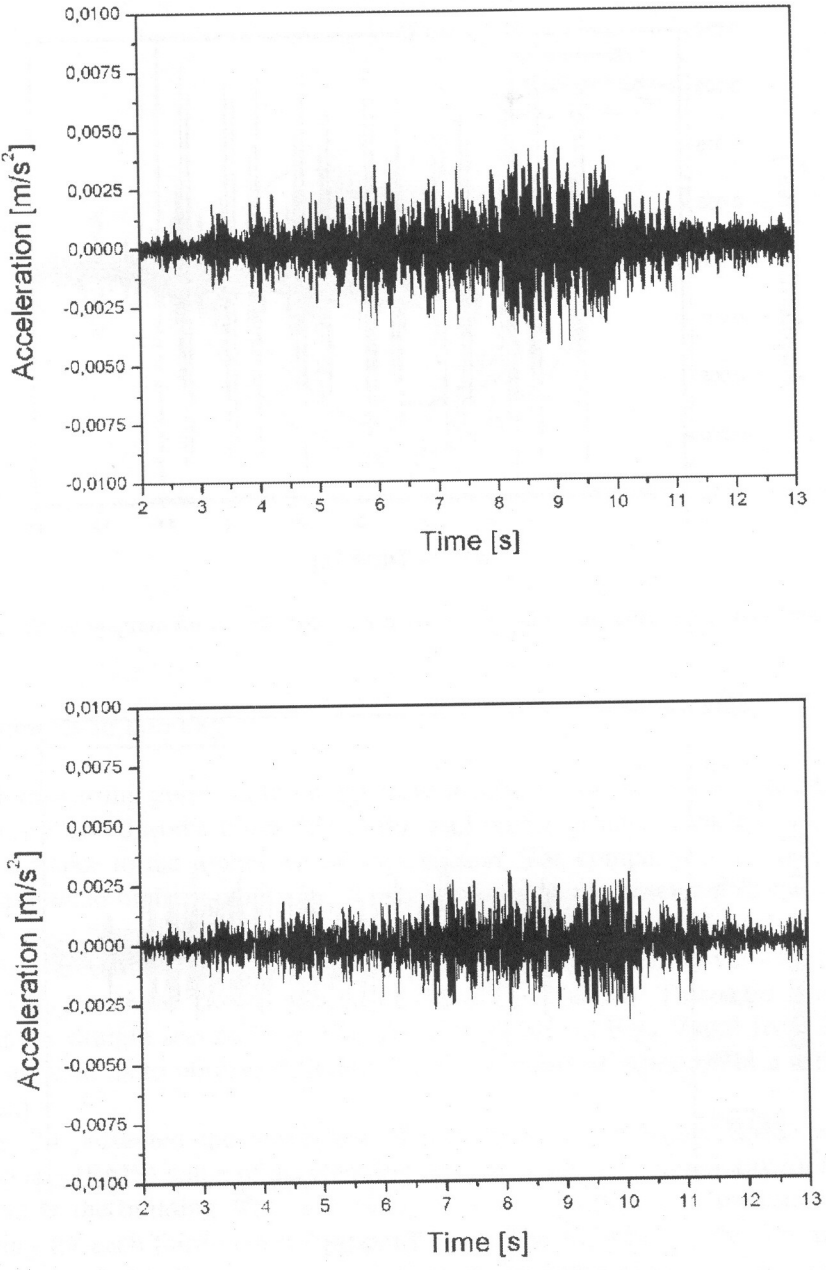

Fig. 17. Time history of vertical (top) and lateral (bottom) accelerations measured on the basement in the building near the straight section of the track

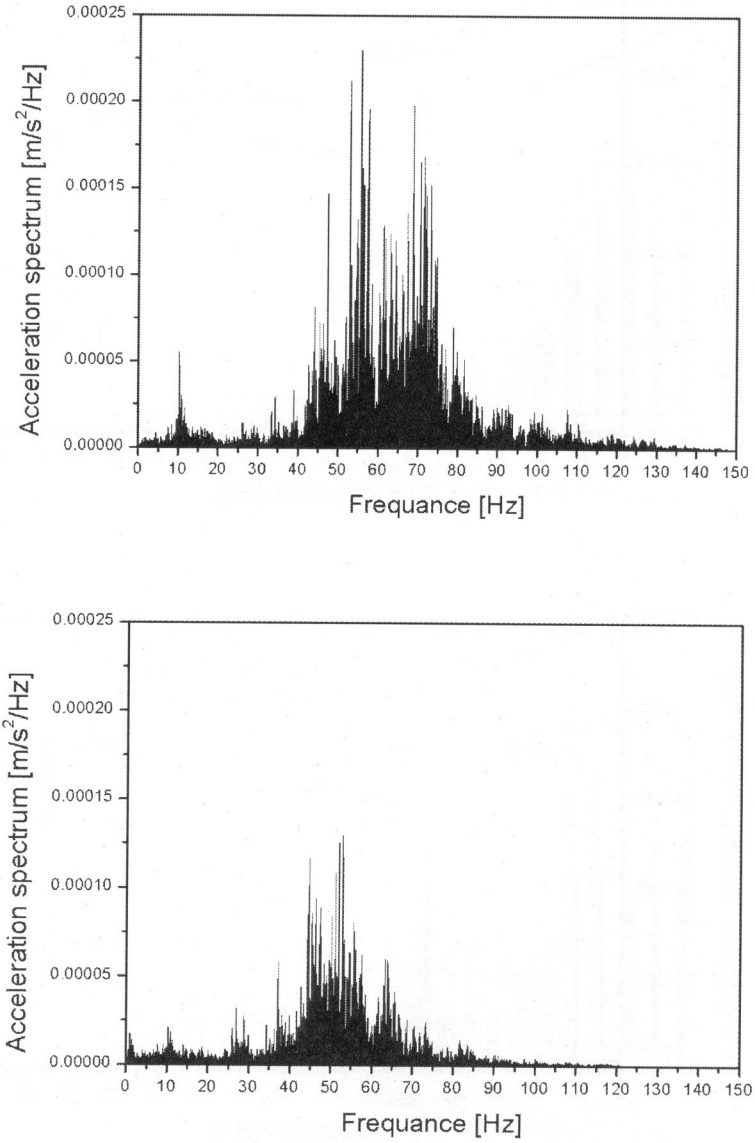

Fig. 18. Magnitudes of the vertical (top) and lateral (bottom) accelerations spectra on the basement in the building near the curved section of the track

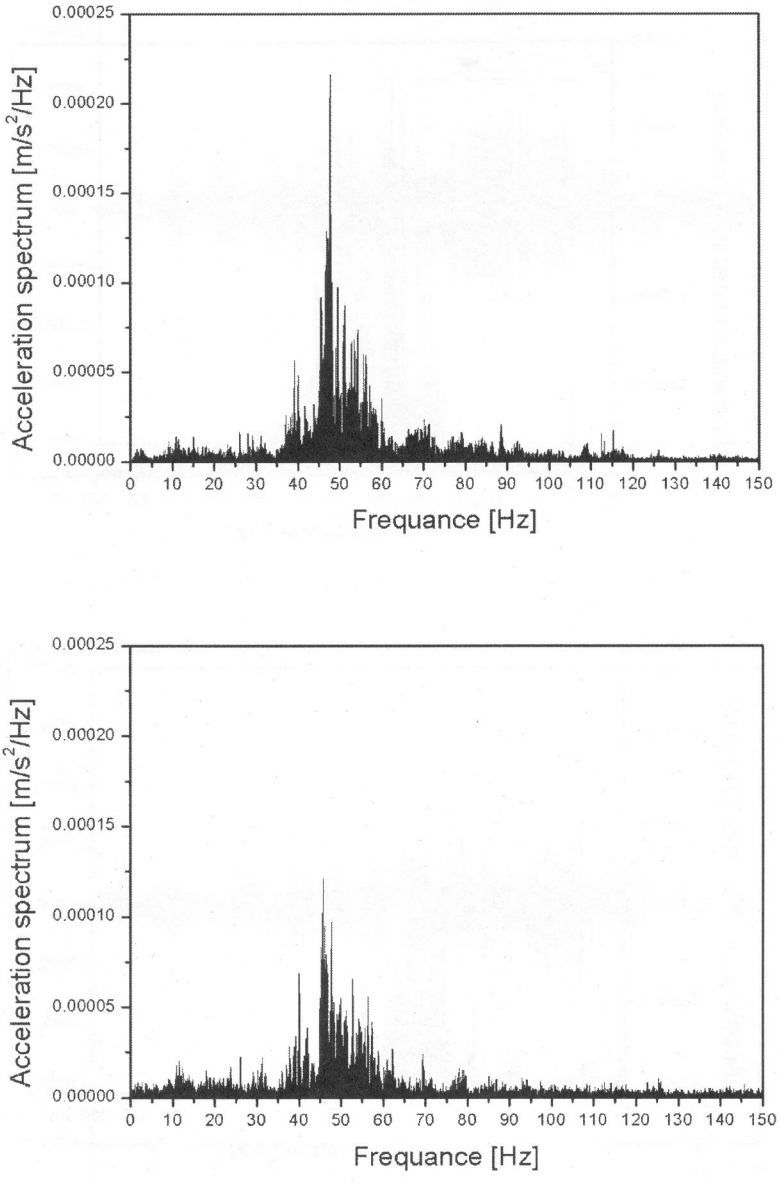

Fig. 19. Magnitudes of the vertical (top) and lateral (bottom) accelerations spectra on the basement in the building near the straight section of the track

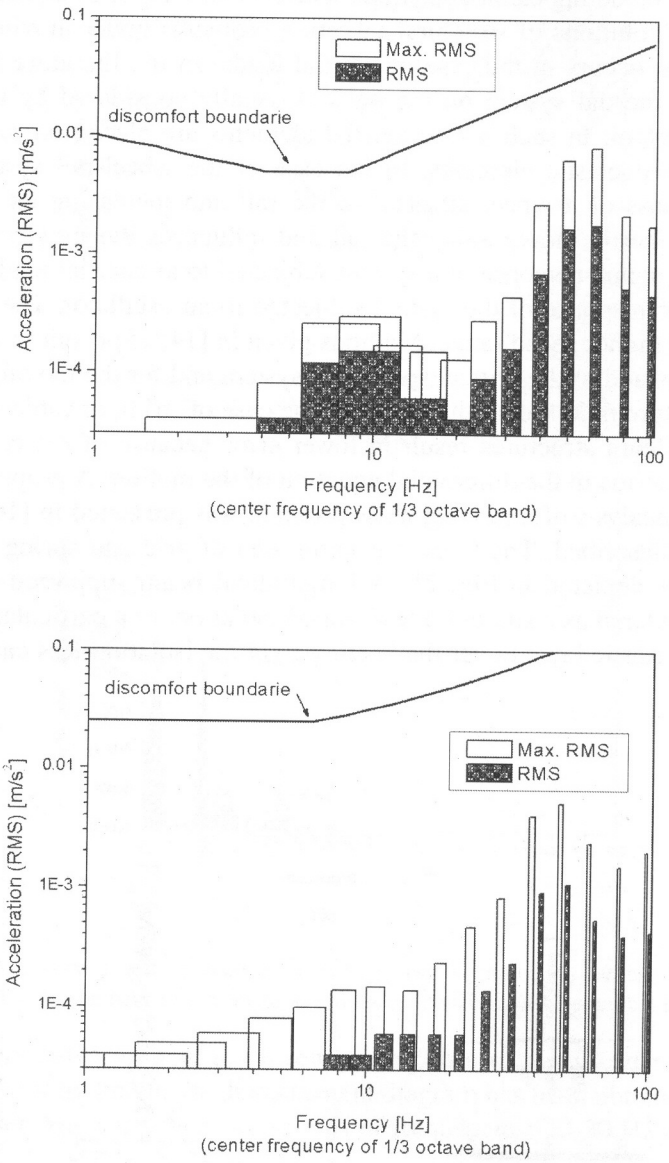

Fig. 20. Diagrams of root mean square and maximum root mean square value of accelerations in vertical (top) and lateral (bottom) direction on the basement in the building near the curved section of the track

3. Numerical Simulation

Numerical modeling cannot be simply performed. First of all commercial codes do not support solutions of structural vibration problems under moving loads. The second problem occurs in the case of inertial loads. In the literature the influence of the moving inertial system on the track is usually considered by introducing a spring-mass system. In such a case inertial elements are placed on rails by means of elastic or viscoelastic elements. In the case of the wheel-rail system we must consider the mass of a wheel attached to the rail and increasing its local inertia. The increased inertia moves along the rail and influences dynamic properties of a system. The dynamic response of a system subjected to an inertial load significantly differs from the response of the system subjected to an oscillator. The difference is significant in a higher speed range. Methods given in [14, 15] result in divergence in higher speed related to the critical speed in a system and for the moving mass to the vibrating structure ratio higher than 0.05. In the case of string or cable systems these methods fail. Beam structures result in lower error because of the contribution of parabolic type terms in the differential equation of the motion. A proper approach to the numerical analysis of a moving mass problem was presented in [16]. We follow the procedure described. The track was composed of grid and spring elements. Its cross-section is depicted in Fig. 21. A longitudinal beam supported on an elastic layer was considered as a solution for vibration isolation. In a particular case of high rigidity of the elastic layer under the beam we get the isolation-less case considered in this paper.

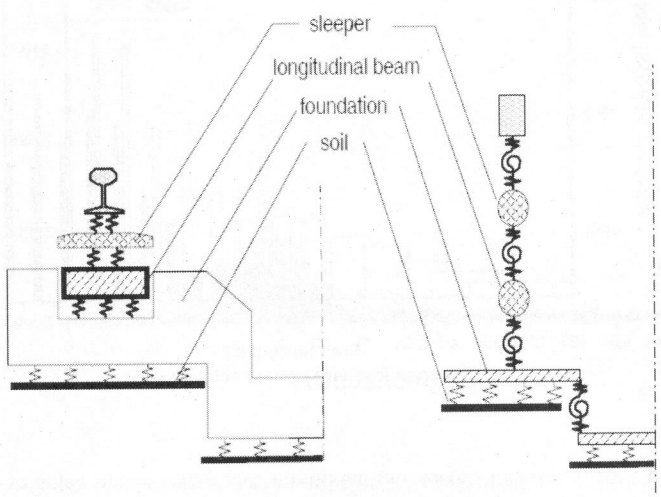

Fig. 21. Cross-section of the model of the track for numerical analysis

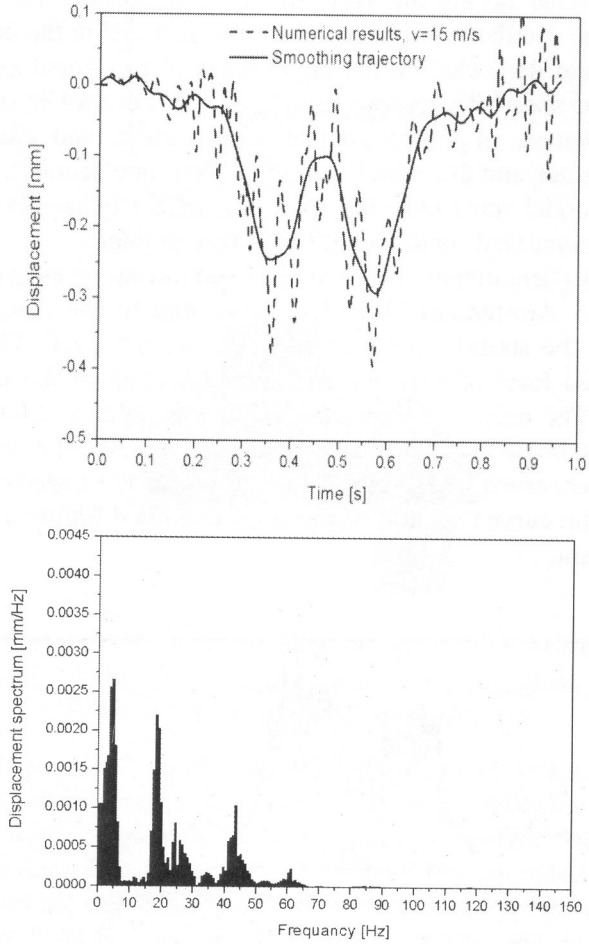

Fig. 22. Time history of vertical displacements (top) and spectra of the vertical displacements (bottom) on the base of a railroad at train speeds v=15 m/s – numerical results

Fig. 22 presented vertical displacement the base of a railroad with numerical simulation. The solid line in the displacement diagram has been obtained by using of a low-pass filter. We can notice two groups of frequencies: 20-30 Hz and 40-50 Hz.

4. Conclusions

In the paper we demonstrated high amplitudes of lateral vibrations in rolling of the wheel over the rail on the underground track. This is an unexpected phenomenon, since intuitively we expect the significant influence of the vertical component of the

acceleration on the environment. Measurements in a real scale were confirmed on the experimental stand during the skew rolling. The motion was characteristic of the double-periodic oscillations. Phase trajectories differed in the case of increasing contact pressure and depended on the angle between the wheel axle and the track axis, and the rolling speed. The proper numerical model cannot be simply elaborated. Both local phenomena, as rolling contact with friction, and global, as dynamic interaction of the track and the vehicle, must be taken into account. Finally resulting response of the model must coincide with real object behaviour. In practice the validation of the numerical model would be a real problem.

The discussed phenomenon was also observed during investigation of the noise of the tram-car in Amsterdam [17]. The noise due to the passage of the tram was measured on the straight and curved section of the track. The measurements presented increased level of noise on the curved section of the track than on the straight of track. The noise exhibited in Fig. 23 was registered with a microphone mounted under the bogie at the first axle of the rail vehicle. The research confirmed the phenomenon observed in the metro tunnel and in the experiment in our case: the vibration on the curved section of the track exhibited higher amplitude than on the straight segment.

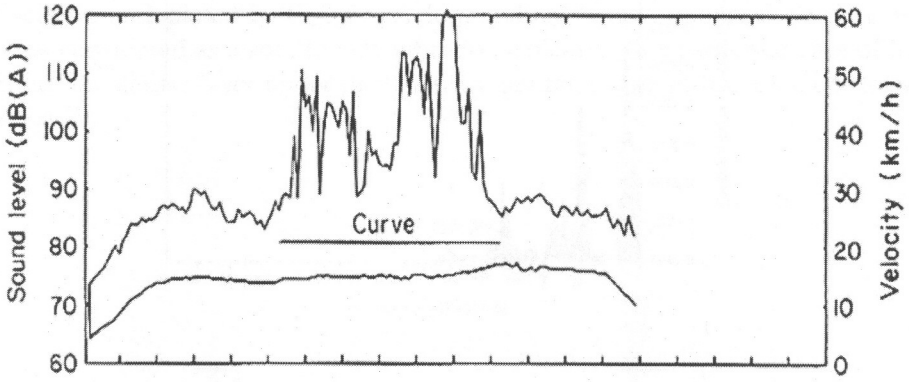

Fig. 23. Time history of A-weight sound level under the rail vehicle and the rolling speed of the vehicle [17]

Several factors influence the amplitude level. We can indicate the wear of railway track caused by centrifugal forces, influenced by the passages of the train, deformations of wheels and wheel rims, wheelsets and rails, interaction of wheel rims with a head of rails (Fig. 24 a), different linear velocity of wheels on curves and rotary oscillations of wheelsets, the plane of the wheel skew with the direction of the rolling resulted in lateral slip in rail/wheel contact zone, and a contact between the rail foot and the base of the fastening system caused by centrifugal forces influenced by the passages of the train (Fig. 24 b).

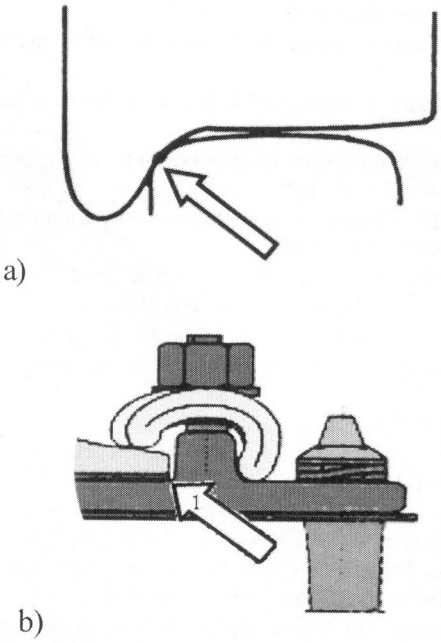

Fig. 24. Contact between the wheel rim and the head of rails (a), point of the contact between the rail foot and the base of the fastening system (b)

The experimental results proved higher amplitudes of vibrations on curves of the track than on straight segments. The lateral slip in rail/wheel contact zone is considered as a possible reason of such a phenomenon. Two frequencies affected the lateral motion. Low frequency motion (1-3 Hz) was generated by the contact of the wheel rim with the rail head and could be influenced by the car body motion. Higher frequency(20-60 Hz), exhibited in the acceleration plot, was affected by the influence of the friction on the relative lateral motion of the wheel and the rail.

The rolling of the wheelset on the track is complex. We can indicate the influence of selected factors on the spurious motion and the wear. The interaction between all factors vary at the straight and curved track. Further intensive works should determine quantitatively the influence of the underground train on the environment.

References

1. Heckl M., Hauck G., Wettschureck R.: Structure-borne sound and vibration from rail traffic. J. Sound and Vibr., 193:175-184, 1996.
2. Konowrocki R., Bogacz R., Bajer Cz.: Study of wheel/road interaction with lateral slip. Simulation in R&D. M. Nader and A. Tylikowski, (Eds), Warsaw, 2005.
3. Bogacz R., Bajer Cz.: Rolling contact with wave phenomena. – Numerical investigation. [In:] Proc.of VIII Pan-American Congress of Applied Mechanics. Havana, pp. 346-349, Cuba, 2004.

4. Melke J.: Noise and vibration from underground railway lines: proposal for a prediction procedure. J. Sound and Vibr., 120(2):391-406, 1988.
5. Lang J.: Ground-borne vibration caused by trams and control measures. J. Sound and Vibr., 122:407-412, 1988.
6. Krylov V.V.: Vibration impact of high-speed trains. J. of Acoustic Society of America, 100(5): 3121-3134, 1996.
7. Krylov V.V.: Effects of track properties on ground vibrations generated by high-speed trains. Acustica-Acta Acustica, 84(1):78–90, 1998.
8. Sheng X., Jones C., Petyt M.: Ground vibration generated by a load moving along a railway track. J. Sound and Vibr., 228(1):129–156, 1999.
9. Bahrekazemi M.: Train-induced ground vibration andi its prediction, Division of Soil and Rock Mechanics, Royal Institute of Technology, Stockholm 2004.
10. Lombaert G., Degrande G., Vanhauwere B., Vandeborght B., Francois S.: The control of ground-borne vibrations from railway traffic by means of continuous floating slabs, J. Sound and Vibr., 297:946–961, 2006.
11. Kuo K.A., Jones S., Hunt H.E.M., Hussein M.F.M.: Applications of PiP: Vibration of embedded foundations near a railway tunnel. [In:] The 7th European Conference on Structural Dynamics (EURODYN), Southampton, UK, 7th-9th of July 2008.
12. Konowrocki R., Bajer Cz.: Investigation of the friction phenomenon in the wheel-road interaction. XXII Symposium: Vibrations in physical systems, 12:173-178, 2006.
13. Konowrocki R.: Wheel-road interaction with lateral slip. PhD thesis. Institute of Fundamental Technological Research, Polish Acad. Sci., 2007 (in Polish).
14. Ting E.C., Genin J., Ginsberg J.H.: A general algorithm for moving mass problems. J. Sound and Vibr., 33(1):49-58, 1974.
15. Filho F.V.: Finite element analysis of structures under moving loads. Shock and Vibration Digest. 10(8):27-35, 1978.
16. Bajer C.I., Dyniewicz B.: Space-time approach to numerical analysis of a string with a moving mass. Int. J. Numer. Meth. Engng., DOI: 10.1002/nme.2372, 2008.
17. van Ruiten C.J.M.: Mechanism of squeal noise generated by tramps. J. Sound and Vibr., 120(2):245-253, 1988.